Monthly Notices
of the
ROYAL ASTRONOMICAL SOCIETY

MNRAS **509,** 3515–3522 (2022)
Advance Access publication 2021 October 25

https://doi.org/10.1093/mnras/stab2992

Direct measurements of infrared intensities of HCN and H_2O + HCN ices for laboratory and observational astrochemistry

Perry A. Gerakines,[1] Yuki Y. Yarnall[1,2] and Reggie L. Hudson[1]★

[1]*Astrochemistry Laboratory, NASA Goddard Space Flight Center, Greenbelt, Maryland 20771, USA*
[2]*Universities Space Research Association, Greenbelt, Maryland 20771, USA*

Accepted 2021 October 11. Received 2021 October 9; in original form 2021 September 12

ABSTRACT

Hydrogen cyanide (HCN) is found in a wide variety of extraterrestrial environments within and beyond the Solar system, and for that reason laboratory spectroscopists have studied this compound in many spectral regions, including the infrared (IR). However, one aspect that remains to be investigated is the intrinsic IR spectral intensities of solid HCN as opposed to relative band strengths, intrinsic intensities being needed to measure HCN abundances. Here we report measurements of IR absorption coefficients and band strengths, along with supporting refractive indices and densities, of both amorphous and crystalline HCN at two temperatures, one for interstellar work and one more relevant to the outer Solar system. Spectra are presented at both temperatures, along with optical constants that can be used in numerical models. Despite widespread and longstanding interest in and investigations of solid HCN, this is the first time that the properties we are reporting have been measured in a single laboratory, avoiding the need for estimates or to combine results from various authors. We find that our measured band strength of $\sim 1 \times 10^{-17}$ cm molecule^{-1} for the C≡N vibration of HCN, in both amorphous HCN and in an H_2O-rich ice, is substantially higher than an earlier estimate. Unless errors of 100 per cent can be tolerated, then our new value requires a rescaling of earlier work. Our results shed light on why HCN and other nitriles have been so difficult to identify in the solid state, in contrast to their many detections in the gas phase.

Key words: astrochemistry – methods: laboratory: atomic.

1 INTRODUCTION

While writing and publishing a paper here 3 yr ago on infrared (IR) spectral assignments in interstellar ice analogues, we were surprised at the difficulty of finding a mid-IR transmission spectrum of amorphous hydrogen cyanide (HCN) near 10 K, a temperature often used by laboratory astrochemists studying interstellar ices. We found it even harder to locate work in which IR spectral intensities for HCN ices were reported, such results being needed to derive molecular abundances from observations. Harder still was locating a conventional IR transmission spectrum of HCN in H_2O-ice, the most abundant interstellar-ice component. Thus motivated, we now address all of these problems, presenting IR transmission spectra of amorphous HCN near 10 K and reporting IR band strengths as well as the density and refractive index measurements on which they are based. We also present spectra of crystalline HCN for comparison to earlier results, addressing a conflict between two different spectra in the literature. We then extend this IR work to spectra of amorphous H_2O + HCN ice mixtures near 10 K for a direct measurement of the IR intensity of one of the mixed ice's HCN bands, which can be used both for astronomical and laboratory studies. Finally, we address the challenge of IR detections of hydrogen cyanide and other nitriles (i.e. −C≡N containing molecules) in extraterrestrial environments.

Hydrogen cyanide is the smallest stable member of the nitrile family, which is the largest class of interstellar molecules identified to date. It was one of the first interstellar molecules found (Snyder & Buhl 1971), it has been observed in comets (e.g. Huebner, Snyder & Buhl 1974; Schloerb et al. 1986; Cordiner et al. 2019), it has been identified in atmospheres of planets such as Pluto (Lellouch et al. 2017) and Jupiter (Tokunaga et al. 1981) and it has been observed in an external galaxy (Brouillet & Schilke 1993) and an exoplanet (Swain et al. 2021). Most such detections have been with radio techniques, but with infrared also being useful, and nearly all such work has concerned the gas-phase molecule. The exception is the IR identification of HCN-ice in Titan's atmosphere, the strongest identification of any solid nitrile there, the HCN assignment having been made by matching two IR bands in Cassini data with our laboratory measurements (Moore et al. 2010; de Kok et al. 2014). Interstellar solid HCN has yet to be identified, which raises the question of whether its IR features are too weak for a detection or whether the HCN abundance is too small for a reliable identification. We address both possibilities in this paper.

Key quantities in all IR laboratory studies of solid HCN, either as a reactant or a product, are the intensities of IR peaks and the strengths of IR absorbance bands. However, although laboratory measurements have reported band positions and widths, few quantitative results are available on intensities. Uyemura & Maeda (1972) reported IR intensities of crystalline HCN at 75 K, but the details of how ice thicknesses were measured were not stated, nor were ranges for band integrations, hindering the work's verification and use. Masterson &

★ E-mail: reggie.hudson@nasa.gov

Published by Oxford University

Khanna (1990) later examined crystalline HCN at 60 K with an eye toward planetary applications, but the coarseness (resolution) of their data table reduces the value of their results. Also, their ice's thickness was determined through an estimate based on liquid HCN.

Turning to amorphous HCN, Moore et al. (2010) published optical constants $n(\nu)$ and $k(\nu)$ of solid HCN at 50 K, a temperature of ices of the outer Solar system. Infrared spectra were recorded with 2-cm^{-1} resolution and analysed with an iterative Kramers–Kronig routine. From the published results it is possible to compute intensities of individual IR peaks, but not IR band strengths unless an ice density is assumed. To our knowledge, neither the published optical constants of Moore et al. (2010), nor the reference refractive index used to derive them, have been verified.

Laboratory work by Bernstein, Sandford & Allamandola (1997) followed a different approach. Those authors condensed an H_2O + HCN (∼10:1) gas-phase mixture to give an amorphous ice at 12 K. By assuming that the intensities of the H_2O features were unchanged from those of neat H_2O (Hudgins et al. 1993), a band strength for the C≡N stretch of HCN was found simply by ratioing against an H_2O-ice feature's IR intensity, an accuracy of 20 per cent being claimed.

Contrasting with this relatively small number of papers on IR intensities of solid HCN is a much larger number of studies that adopted one HCN value or another in a study of low-temperature reaction chemistry. From this journal alone, at least four such studies can be cited. Fresneau et al. (2015) examined reactions of HCN and acetaldehyde, adopting the Bernstein et al. (1997) value for the intensity of HCN's fundamental band near 2100 cm^{-1}. Rachid et al. (2021) used the same band strength in a study of the radiolytic formation of HCN and other small molecules. Fedoseev et al. (2018) used a different HCN band strength in their study of the synthesis of HCN and other products in N_2-containing interstellar ice analogues. The value adopted came from the work of Moore & Hudson (2003) on a band strength measured with a different method and that gave a different result from that of Bernstein et al. (1997). Finally, Noble et al. (2013) studied a solid-phase acid-base reaction of NH_3 with HCN, adopting a band strength for the HCN fundamental, again near 2100 cm^{-1}, which differs from that used by the other authors just cited.

Moving beyond this journal, it is just as easy to find just as many publications that used a variety of HCN infrared band strengths. Wu et al. (2012) eschewed laboratory measurements and relied on a density-functional calculation in their HCN work. Theule et al. (2011) examined H_2O-free HCN-containing ices and used the band strength for an H_2O-rich solid published by Bernstein et al. (1997), as did Jimenez-Escobar et al. (2014) and Danger et al. (2014). Jamieson, Chang & Kaiser (2009) appear to have adopted a band strength from an unchecked gas-phase calculation. A paper from the same group (Quinto-Hernandez et al. 2011) cited Hassner et al. (1990) for a band strength of HCN (with incorrect units), but the latter work is not concerned with hydrogen cyanide and it does not give a band strength for that compound.

In short, the situation with HCN resembles that which we encountered in our recent papers here on aldehydes (Hudson & Ferrante 2020; Yarnall, Gerakines & Hudson 2020). Infrared peak positions and band widths have been reported for solid HCN, but not the IR spectral intensity information necessary to quantify studies of this molecule in extraterrestrial ices and their laboratory analogues. Therefore, here we report IR intensity measurements that are needed to quantify all such work, either directly or indirectly. Specifically, we are reporting absorption coefficients and band strengths of HCN ices in which the underlying densities and refractive indices also have been measured. Results are given for two forms of HCN, amorphous and crystalline, along with IR optical constants of each. We present our optical constants in tables, figures, and in electronic form. We emphasize that this is the first reasonably comprehensive IR investigation of HCN ices of its type, covering both the infrared measurements and the underlying work needed to better quantify them. Finally, we present the first direct measurement of an IR band strength of HCN in an H_2O + HCN ice.

2 EXPERIMENTAL SECTION

The procedures followed and equipment used were almost identical to those in our recent publications in this journal (Hudson & Ferrante 2020; Yarnall et al. 2020), so only differences will be described. The most significant difference was that we prepared the title compound, HCN, instead of purchasing it. The method was essentially that of Gerakines, Moore & Hudson (2004) in which potassium cyanide and an excess of stearic acid (octadecanoic acid) were warmed slowly on a vacuum line to generate HCN, as in equation (1) below.

$$C_{17}H_{35}COOH + KCN \rightarrow C_{17}H_{35}COOK + HCN \uparrow \quad (1)$$

Water was removed from the HCN product in equation (1) by passage over P_2O_5. The HCN was further purified by freezing at −116 °C in an ethanol-liquid-N_2 slush bath and pumping to remove any CO_2. Starting materials were purchased from Sigma Aldrich.

As before, IR spectra were recorded as 100-scan accumulations with a Thermo iS50 spectrometer (DTGS detector) at a resolution of 1 cm^{-1} from 5000 to 500 cm^{-1}. Ice samples were again made by vapor-phase deposition onto a pre-cooled CsI substrate, either near 10 K for amorphous HCN or at 120 K for crystalline ices. (The minimum temperature varied from 9 to 13 K during this work, but for convenience we use 10 K throughout this paper.) Our earlier publication here (Yarnall et al. 2020) has additional details such as for the measurement of each ice sample's thickness, refractive index at 670 nm (n_{670}), and density (ρ, g cm^{-3}). Two-laser interferometry gave refractive indices and a quartz-crystal microbalance gave densities (e.g. Satorre et al. 2008; Hudson, Loeffler & Gerakines 2017; Hudson et al. 2020). The usual Beer's Law plots of IR absorbance-peak height as a function of ice thickness (h) gave apparent absorption coefficients (α'), while plots of IR absorbance-band area as a function of ice thickness gave apparent band strengths (A'). The relevant equations are (2) and (3) below, where ρ_N is number density. Errors and uncertainties for A' and α' are discussed in Hudson et al. (2017) and are ∼5 per cent, and less for the stronger IR features.

$$Absorbance = \left(\frac{\alpha'}{2.303}\right) h, \quad (2)$$

$$\int_{\text{band}} (Absorbance)\, d\tilde{\nu} = \left(\frac{\rho_N A'}{2.303}\right) h. \quad (3)$$

Our method for measuring the band strength of the C≡N stretch of HCN in an H_2O-ice requires comment. After measuring the density and refractive indices of HCN and H_2O (*vide infra*), we used those results to calibrate the condensation rate of HCN and H_2O after each gas or vapour passed through a leak valve and deposition line leading to our pre-cooled substrate. Knowing the HCN deposition rate was equivalent to knowing the flux (molecules cm^{-2} sec^{-1}) of HCN condensing on the substrate. Multiplying this flux by the deposition time (s) gave the column density (molecules cm^{-2}) of HCN in the ice, which was the same as the product '$\rho_N\, h$' in equation (3). An IR spectrum of each such ice formed gave a data set consisting of HCN column densities and corresponding IR band areas. Plotting

Table 1. Refractive indices and densities of nitrile ices[a]

Ice	Form	T / K	n_{670}	ρ / g cm^{-3}
Hydrogen cyanide HCN	amorphous	18	1.346	0.850
Hydrogen cyanide HCN	crystalline	120	1.428	1.037
Acetonitrile CH_3CN	amorphous	15	1.334	0.778
Propionitrile CH_3CH_2CN	amorphous	15	1.311	0.703

Note. [a]See the text for uncertainties. An extra significant figure has been carried for a few values.

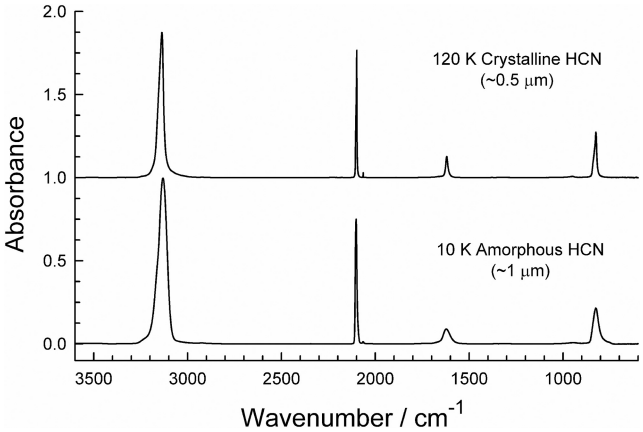

Figure 1. Mid-IR spectra of amorphous and crystalline HCN prepared by vapour-phase deposition onto a CsI substrate at 10 K and 120 K, respectively. Note that the ice thicknesses were ~1 μm for the amorphous ice, but only ~0.5 μm for the crystalline ice. The spectra are offset for clarity.

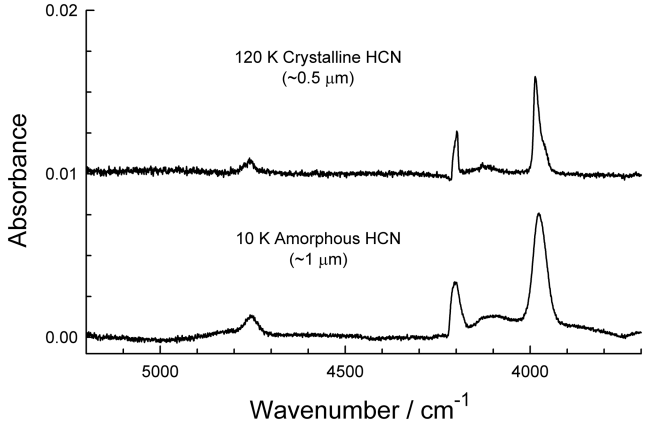

Figure 2. Near-IR spectra of amorphous and crystalline HCN prepared by vapour-phase deposition onto a CsI substrate at 10 K and 120 K, respectively. Note that the ice thicknesses were ~1 μm for the amorphous ice, but only ~0.5 μm for the crystalline ice. The spectra are offset for clarity.

such data according to equation (3), the integral in (3) against HCN column density ($\rho_N h$), gave points that fell along a straight line, with a slope that was simply (A'/2.303), from which A' was readily found. An example is given in the next section.

3 RESULTS

3.1 Densities and refractive indices–HCN

Accurate values of a reference refractive index (n_{670}) were critical for measurements of ice thickness, which in turn were needed for extracting IR intensities from our spectra and for the calculation of optical constants. Measurements of density (ρ) also were needed for band-strength determinations. For this study we measured n_{670} and ρ in triplicate or more for amorphous HCN at 18 K and crystalline HCN at 120 K. Average values are given in Table 1, along with results for two other compounds to which we return in our Discussion. Standard errors for n_{670} and ρ were about $\pm$ 0.005 and $\pm$ 0.005 g cm^{-3}, respectively.

3.2 Infrared spectra–HCN

Fig. 1 shows mid-IR survey spectra of solid HCN at 10 K (amorphous ice) and 120 K (crystalline ice), with the latter vertically offset for clarity. Weaker IR features at higher wavenumbers (smaller wavelengths) are shown in Fig. 2. These spectra are free of interferences from solid H_2O and CO_2, common laboratory contaminants, and are qualitatively similar to those published by others (e.g. Moore et al. 2010), allowing for differences in temperature and the way the spectra were obtained. We recorded IR spectra of HCN ices at 10 and 120 K with at least four different thicknesses, from about 0.25 to 3 μm, covering at least six samples. Peak heights and band areas of spectra were measured, and the usual Beer's Law plots were prepared in accordance with equations (2) and (3). See Fig. 3 for examples. The results of such work led to the IR intensities, α' and A', in Tables 2 and 3. We emphasize that it is important to include integration ranges in such tables to aid in the application of measured IR intensities and to assist in lab-to-lab comparisons.

In addition to measuring intensities α' and A', we also have calculated the optical constants $n(\nu)$ and $k(\nu)$ of amorphous and crystalline HCN. Our recent paper (Gerakines and Hudson 2020) describes our method in detail and makes our open-source software available in two different versions. Figs 4 and 5 show the HCN optical constants we calculated using an iterative Kramers–Kronig routine. Our own experience is that such graphs can be illustrative of optical constants, but in practice they are of limited use. Therefore, we have placed all of our $n(\nu)$ and $k(\nu)$ values on our group's webpage at https://science.gsfc.nasa.gov/691/cosmicice/constants.html. These optical constants can be used with the equations of either Tomlin (1968) or Swanepoel (1983) to generate IR spectra in either a transmission or a reflection mode.

3.3 Infrared spectra–H_2O + HCN

A question that is sometimes asked concerns the extent to which the IR band strengths of a compound change when it resides in an amorphous H_2O-ice. In the case of solid HCN, the relevant laboratory results consist of a single measurement for an H_2O + HCN ice from Bernstein et al. (1997). Those authors combined H_2O and HCN in a 10:1 ratio in a gas bulb, and then condensed the resulting mixture onto a pre-cooled substrate with methods similar to those used in our own work. An underlying, and common, assumption was that

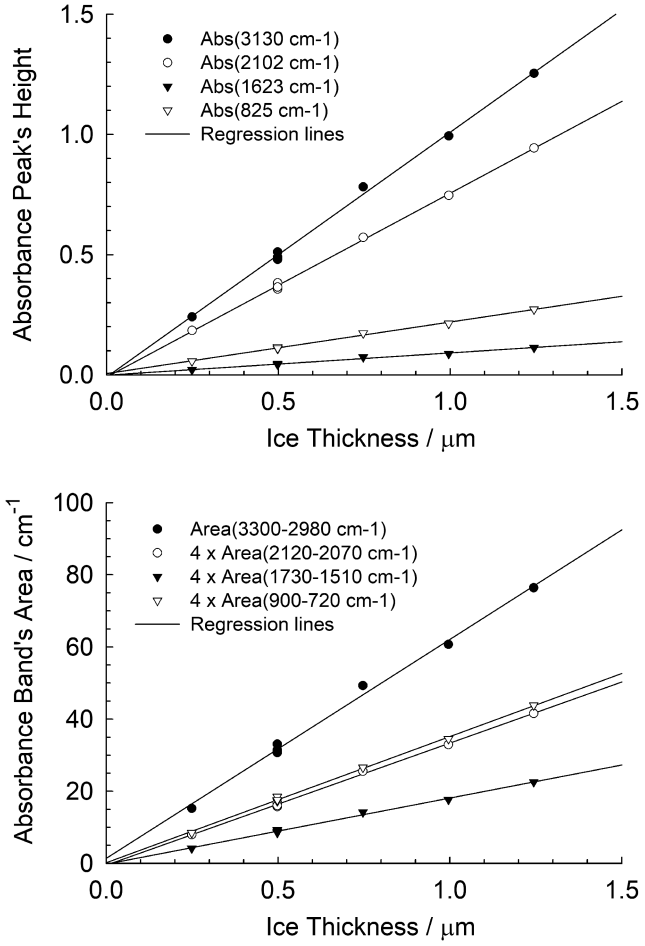

Figure 3. Representative Beer's Law plots for the determination of apparent absorption coefficients (α') and band strengths (A') for four IR features of amorphous HCN at 10 K.

the gas-phase mixture and the solid-phase ice had the same H_2O-to-HCN ratio.

To avoid making the assumption just described, we prepared H_2O + HCN ices with the two compounds being deposited at 10 K from *separate* gas bulbs each equipped with its own adjustable leak valve and deposition line. To make such a two-component mixture, and later to analyse the results, we first had to calibrate the deposition rates for H_2O and HCN onto our CsI substrate. This was straightforward for amorphous HCN given the results of Tables 1 and 2, but the H_2O calibration proved slightly more challenging because a refractive index and a density for amorphous H_2O were needed and the most appropriate values to use were not obvious. For example, the lowest density we have seen is ∼0.6 g cm^{-3} for amorphous H_2O-ice near 22 K made by background deposition (Dohnálek et al. 2003). A slightly higher value is from Westley, Baratta & Baragiola (1998), 0.82 g cm^{-3} from 30 to 135 K. Hudgins et al. (1993) assumed, perhaps for simplicity, a density of amorphous H_2O-ice of 1 g cm^{-3} at 10 K, and Venkatesh, Rice & Narten (1974) reported 1.2 g cm^{-3}. Faced with these choices based on estimates, assumptions, and extrapolations to our work, and potential objections to each, we decided to measure n and ρ for amorphous H_2O-ice with the same equipment used for the HCN results in Table 1. Averages of four measurements gave $n_{670} = 1.234 \pm 0.008$ and $\rho = 0.719 \pm 0.005$ g cm^{-3} at 19 K. These were the values used to calibrate our H_2O depositions to make H_2O + HCN ices.

With our n_{670} and ρ values in hand, we calculated H_2O and HCN condensation rates that gave ices with approximate molecular ratios of H_2O: HCN = 10:1, 20:1, and 50:1, four ices (i.e. four different thicknesses) for each ratio. After preparing each ice, recording its IR spectrum, and integrating the HCN band near 2100 cm^{-1} in each case, and knowing the number density of HCN in each sample (Section 2), we graphed the data as described earlier. Fig. 6 shows the result. The slope, on multiplying by 2.303, gave A'(10 K HCN, 2100 cm^{-1}) = 1.12×10^{-17} cm molecule^{-1}, about 120 per cent larger than the literature value of A'(10 K HCN, 2092 cm^{-1}) = 5.1×10^{-18} cm molecule^{-1} (Bernstein et al. 1997).

As a check on our work we plotted the IR intensity of the C≡N band of our H_2O + HCN ices (50:1, 20:1, 10:1) as a function of ice thickness, and then used equation (3) to determine A'. This required us to choose an ice density, and so we assumed the same value as for H_2O alone. The average C≡N band strength from this estimate was 1.1×10^{-17} ($\pm 0.1 \times 10^{-17}$) cm molecule^{-1}, essentially the same as the value obtained by measuring deposition times.

We have found it difficult to locate conventional transmission IR spectra of H_2O-rich ices containing HCN, and so in Fig. 7 we present an IR spectrum of an amorphous ∼20:1 H_2O + HCN ice mixture at 10 K. The position (2092 cm^{-1}) and width (18 cm^{-1}) of our HCN band agree with those of Bernstein et al. (1997), who showed a transmission spectrum of their H_2O + HCN ice, but only from 2250 to 2050 cm^{-1}. Also, the position, intensity, and shape of the C≡N band in our spectra scarcely change on warming the amorphous mixture to 120 K. Gerakines et al. (2004) showed the spectrum of a 5:1 H_2O + HCN mixture at 18 K, but the reflection mode used can distort IR intensities. The same comment applies to the IR spectrum of a 2.5:1 H_2O + HCN mixture at 40 K from Danger et al. (2014).

4 DISCUSSION

4.1 Densities and refractive indices

There are few published results with which to compare our values of n_{670} and ρ of amorphous and crystalline HCN (Table 1). We know of no published density for amorphous HCN, but Moore et al. (2010) reported $n_{670} = 1.30 \pm 0.02$ at 30 K, which is almost within experimental error of our results, but slightly lower. For crystalline HCN, Masterson & Khanna (1990) used the Lorentz–Lorenz equation and data from liquid HCN to calculate $n = 1.36$ (no wavelength given), considerably lower than our 1.428. The best comparison we have found for our results is to the density of crystalline HCN from the X-ray diffraction work by Dulmage & Lipscomb (1951). Those authors reported $\rho = 1.03$ g cm^{-3} near 153 K, in excellent agreement with our $\rho = 1.037$ g cm^{-3} at 120 K. These results show that our HCN prepared at 120 K had a very high degree of crystallinity.

4.2 Infrared spectra

The IR peak positions of HCN in our figures and tables agree well with those in the literature, including the shift of about 34 cm^{-1} for the ^{13}C satellite peak near 2065 cm^{-1}. See the papers already cited. Pézolet & Savoie (1969) reported peak positions for two crystalline forms of HCN, with a transition temperature at 170 K. A comparison of our results at 120 K with their work suggests that our crystalline HCN was in the low-temperature form, as expected.

Table 2. Intensities of selected IR absorptions of amorphous HCN at 10 K[a]

Assignment[b]	Peak position/cm^{-1}	α'/cm^{-1}	Integration range/cm^{-1}	A'/10^{-18} cm molecule^{-1}	Approximate description[b]
$2\upsilon_2 + \upsilon_1$	4754	14	4777–4716	0.026	combination
$2\upsilon_3$	4202	51	4231–4130	0.088	overtone
$\upsilon_1 + \upsilon_2$	3975	144	4018–3920	0.32	combination
υ_1	3130	23400	3300–2980	73.84	C–H stretch
υ_3	2102	17600	2120–2070	10.29	C≡N stretch
$2\upsilon_2$	1623	2130	1730–1510	5.57	overtone
υ_2	825	4940	900–720	10.64	HCN bend

Notes. [a]Ice thicknesses were calculated using $n_{670} = 1.346$. Most values of α' and A' are rounded to three significant figures. An extra significant figure has been carried for a few values of A'. See the text for uncertainties.
[b]Assignments for peak positions higher than 4000 cm^{-1} are more tentative than for other features. Other ways to number the HCN vibrations in the first column can be found in the literature.

Table 3. Intensities of selected IR absorptions of crystalline HCN at 120 K[a]

Assignment[b]	Peak position/cm^{-1}	α'/cm^{-1}	Integration range/cm^{-1}	A'/10^{-18} cm molecule^{-1}	Approximate description[b]
$2\upsilon_2 + \upsilon_1$	4754	31	4790–4738	0.031	combination
$2\upsilon_3$	4197	37	4216–4175	0.046	overtone
$\upsilon_1 + \upsilon_2$	3986	278	4005–3930	0.27	combination
υ_1	3136	45600	3260–2980	70.30	C–H stretch
υ_3	2099	39800	2120–2080	10.28	C≡N stretch
$2\upsilon_2$	1620	6250	1750–1520	5.22	overtone
υ_2	826	11900	900–760	10.57	HCN bend

Notes. [a]Ice thicknesses were calculated using $n_{670} = 1.428$. Most values of α' and A' are rounded to three significant figures. An extra significant figure has been carried for a few values of A'. See the text for uncertainties.
[b]Assignments for peak positions higher than 4000 cm^{-1} are more tentative than for other features. Other ways to number the HCN vibrations in the first column can be found in the literature.

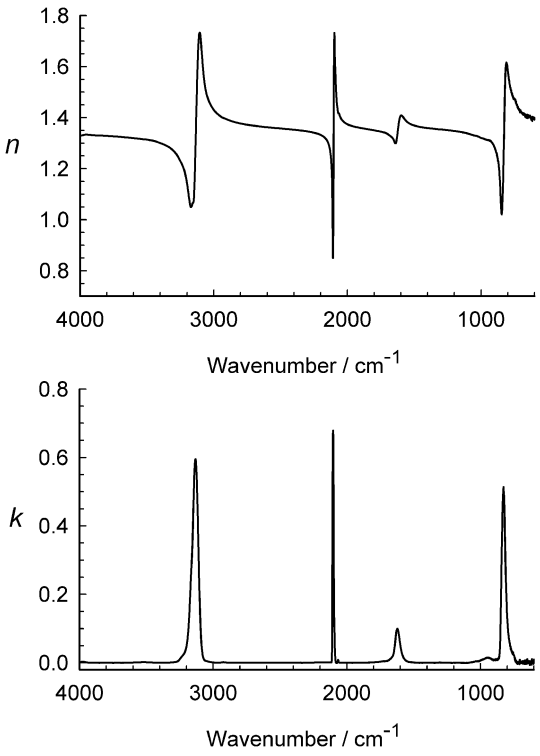

Figure 4. Optical constants for amorphous HCN at 10 K.

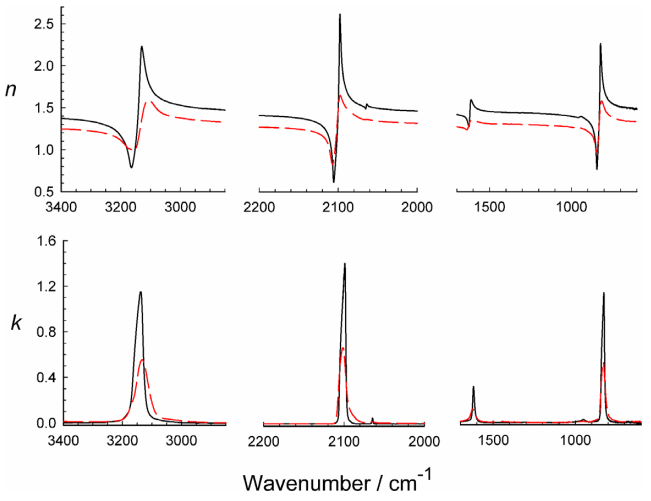

Figure 5. Optical constants for crystalline HCN at 120 K. Data from this work is drawn with a solid black line; data from Moore et al. (2010) is drawn with a broken red line.

What is of more interest here, and more difficult to compare, are IR intensities. For optical constants of amorphous HCN, there is only the paper of Moore et al. (2010). Their optical constants $k(\nu)$ are in excellent agreement with ours, but their values of $n(\nu)$ are about 0.02 lower than those shown in Fig. 4, reflecting the difference in starting (reference) values of n_{670} used. The fact that our amorphous HCN was made at 10 K, but the ice of Moore et al. (2010) was made

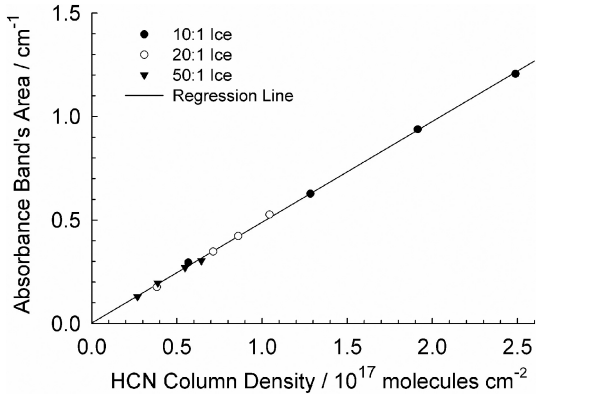

Figure 6. Area of the C≡N band of HCN (∼2100 cm^{-1}) in 12 H_2O + HCN ices having H_2O: HCN ratios of 10:1, 20:1, and 50:1. The temperature was 10 K.

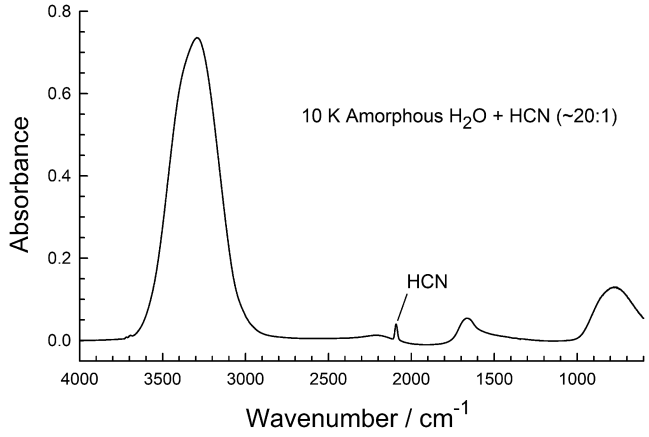

Figure 7. Mid-IR spectrum of an H_2O + HCN (∼20:1) ice at 10 K. The ice's thickness was about 1 μm.

at 50 K, appears to have had little or no influence on the optical constants $n(\nu)$ and $k(\nu)$.

For comparisons involving crystalline HCN, we again turn to the work of Moore et al. (2010). Fig. 5 shows their optical constants for crystalline HCN at 120 K plotted with ours, and significant differences are now seen for both $n(\nu)$ and $k(\nu)$. The differences in the upper graph, for $n(\nu)$, might again be due to different choices for the reference value of n_{670} used in the calculations, but the differences in the lower graph for $k(\nu)$ suggest a second contributing factor. We suspect that the variations seen in $n(\nu)$ and $k(\nu)$ are from differences in sample preparation. Our crystalline HCN ice was made by vapour-phase deposition at 120 K, but that of Moore et al. (2010) was made by warming an amorphous HCN sample to 120 K, a procedure that the authors noted would not give the same degrees of crystallinity as a higher temperature deposition.

A different way to compare our work to that of Moore et al. (2010) is to examine the intensities of IR peaks either through k values at peak positions or through absolute absorption coefficients defined by equation (4).

$$\alpha\ (\tilde{\nu}) = 4\pi\tilde{\nu}k\,(\tilde{\nu})\,. \tag{4}$$

We find that the average deviation of the α (or k) values of the three fundamentals of HCN, between our work and that in Moore et al. (2010), is about 4 per cent for amorphous HCN, but about 40 per cent for crystalline HCN, reflecting the variations seen in Figs 4 and 5. A similar comparison to the results of Masterton & Khanna (1990) for crystalline HCN gives a deviation of about 20 per cent. It is difficult to make more precise comparisons due to the lack of published details such as integration ranges for band strengths in that paper and others (e.g. Uyemura & Maeda 1972; Dello Russo & Khanna 1996).

Yet another comparison comes from looking at our IR results and those from some related molecules, in this case simple nitriles. Moore et al. (2010) published optical constants for CH_3CN and CH_3CH_2CN, and we have used their results, our equation (4), and our nitrile densities of Table 1 to calculate absolute band strengths (A) with equation (5).

$$A = \frac{1}{\rho_N}\int_{\tilde{\nu}_1}^{\tilde{\nu}_2}\alpha\,(\tilde{\nu})\,\mathrm{d}\tilde{\nu}. \tag{5}$$

Integration of the C≡N stretching bands of these three nitriles gives absolute band strengths, in units of 10^{-18} cm $molecule^{-1}$, of 10.3, 2.4, and 2.8 for amorphous HCN, CH_3CN, and CH_3CH_2CN, respectively. Hydrogen cyanide is clearly the strongest absorber of the three. The C≡N vibration, near 2100 cm^{-1}, was chosen for comparison as it probably is the most promising for astronomical observations, being in a region free of obscuration by such common extraterrestrial ice components as H_2O-ice and silicates.

Our main interest here has been IR intensities of amorphous HCN and H_2O + HCN ices, but our work with crystalline HCN sheds light on a small mystery in the literature. Masterton & Khanna (1990) published an IR spectrum of crystalline HCN ice as did Anderson et al. (2018). Peak positions in the two spectra are similar, but there is a striking difference in the relative intensities of IR peaks. For example, the peak near 826 cm^{-1} is less than a third of the height of the peak near 2099 cm^{-1} in Masterton & Khanna (1990), but the two peaks have almost the same height in Anderson et al. (2018). The IR peak near 1620 cm^{-1} is about a sixth of the height of the peak near 2099 cm^{-1} in Masterton & Khanna (1990), but about half as high in Anderson et al. (2018). The reasons for such drastic intensity differences are unknown, but our spectrum of crystalline HCN in Fig. 1 is almost exactly like that of Masterton & Khanna (1990). We also note that the IR spectrum of Anderson et al. (2018) was said to be for an ice with a thickness of 4.29 μm. Using our values of α', we estimate that this would give an absorbance of about 7 (optical depth ∼ 17) near 2099 cm^{-1}, which seems unlikely as it would lead to severe distortion and saturation of all three fundamental bands of HCN. The 4.29-μm thickness might be a typographical error in the Anderson et al. (2018) paper, although that does not explain the anomalous peak intensities. The vertical axis of the spectra of neat HCN in that same paper lacked a numerical scale, making a more quantitative comparison impossible.

4.3 Where have all the nitriles gone?

A question related to HCN solid-phase chemistry concerns why this molecule and other nitriles have not yet been identified in the IR spectra of interstellar ices. Our results show that the IR intensities of the three fundamental bands of HCN are sufficiently strong for detection, but the HCN absorbances near 3130 and 825 cm^{-1} overlap with strong IR bands from H_2O-ice and interstellar silicates, respectively. In contrast, the HCN feature near 2100 cm^{-1} sits in an uncluttered part of the mid-IR spectrum, again with moderate intrinsic intensity. Its non-detection suggests something else that hinders the observation of this solid-phase HCN peak.

We propose that it is not spectroscopy but chemistry that is responsible for the difficulty in finding HCN in interstellar solids. There are several ways in which HCN can be formed in ices, such as by either radiolysis or photolysis of $N_2 + CH_4$ mixtures, and these have been studied by several research groups for applications to Titan. Also, any system in which CH_3NH_2 is formed such as by insertion of CH_2 into an N–H bond of NH_3, also should form HCN by radiation-induced oxidation (i.e. $CH_3NH_2 \rightarrow$ HCN). However, competing with HCN formation are several ways HCN can be consumed, some of which we have described in other papers. We have not found that HCN, a weak acid, reacts with H_2O, the main component of interstellar ices, to any appreciable degree, but NH_3 is a stronger base than H_2O so that the acid-base chemistry of reaction (6) readily occurs in the solid state (Gerakines et al. 2004).

$$HCN + NH_3 \rightarrow NH_4CN \quad (6)$$

Because of equation (6), the formation of HCN from the $N_2 + CH_4$ mixtures already mentioned changes to the formation of the cyanide ion, CN^-, in $NH_3 + CH_4$ mixtures.

Radiolytic and photolytic oxidation are two other paths for HCN consumption. In earlier papers we showed that HCN and many H_2O-rich ices with molecules possessing a $-C\equiv N$ (nitrile) group produce the cyanate ion, OCN^-, on either proton irradiation or far-UV photolysis (Gerakines et al. 2004; Hudson & Moore 2004). The reactions are so efficient that it would be rather remarkable if either HCN or CN^- was found in an H_2O-rich ice exposed to ionizing radiation. One expects to find the sequence in equation (7) in such ices, with OCN^- being hydrolysed to CO_2 in the second step.

$$HCN\ (\text{or } CN^-) \rightarrow OCN^- \rightarrow CO_2 \quad (7)$$

Some other reactions by which the abundance of HCN can be kept low include hydrogenation to make amines, the Strecker rection to produce amino acids, dissociative electron capture ($HCN + e^- \rightarrow H + CN^-$), and O-atom capture to make HNCO (e.g. Crowley & Sodeau 1989; Hudson, Moore & Gerakines 2001).

We conclude that HCN and other nitriles will continue to be difficult to identify in extraterrestrial ices, not because of the weakness of their IR bands, but because of the multiple ways by which such molecules can be destroyed in solids. Environments with little or no H_2O-ice such as Titan are exceptions.

4.4 Applications

Applications of our data are similar to those described in our recent papers here (e.g. Hudson & Ferrante 2020; Yarnall et al. 2020). Our results can be used to quantify laboratory IR experiments involving HCN, either its formation or destruction, our work being the first to be based on ice measurements at each step. Another way our results can be used is as reference data for measuring HCN infrared band strengths in multicomponents ices such as H_2O + HCN as shown in our Section 3.3. So many combinations of variables such as temperature, number, and type of components, and concentrations, exist for such ices that evaluating band strengths for all of them is not feasible. However, our HCN data can be used for calibrations to determine HCN abundances in many types of mixtures. In other words, independent calibrations of the HCN contribution can be made using our data without having to resort to assumptions about the composition of an ice compared to the composition of a gas mixture. Our mid-IR intensities also can be used as a starting point for scaling to determine IR intensities of HCN in the near- and far-IR regions (e.g. Gerakines et al. 2005; Giulano et al. 2014).

Finally, we return again to the widely used band strength of HCN in an H_2O-rich ice, A'(HCN, 2092 cm^{-1}) = 5.1×10^{-18} cm $molecule^{-1}$ from Bernstein et al. (1997). We have shown that this value needs to be raised by about 120 per cent to 1.12×10^{-17} cm $molecule^{-1}$ to match our laboratory measurements. Our work also shows that there is relatively little difference in the C≡N infrared band strength between pure amorphous HCN and HCN embedded in an amorphous H_2O-rich ice.

5 SUMMARY AND CONCLUSIONS

Amorphous and crystalline HCN have been prepared under vacuum near 10 and 120 K, respectively, and the following quantities measured, many for the first time: refractive index at 670 nm, density, mid-IR transmission spectrum, apparent IR absorption coefficients, apparent IR band strengths, and optical constants. An improved method for measuring the strength of HCN's infrared feature near 2100 cm^{-1} in H_2O-ice has been described, and used to update the literature value, the new value being about 120 per cent larger than the old one. The IR band strengths of HCN in the absence and in the presence of H_2O-ice near 10 K are almost the same. The work in this paper is another contribution to our on-going effort to make accurate measurements of such properties for observational astronomy, laboratory astrochemistry, and the interpretation of spacecraft results. With NASA's upcoming Dragonfly mission to Titan, a world known to harbour nitrile ices, we expect that interest in the properties of solid HCN will be of increasing interest.

ACKNOWLEDGEMENTS

We acknowledge the support of NASA's Planetary Science Division Internal Scientist Funding Program through the Fundamental Laboratory Research (FLaRe) work package at the NASA Goddard Space Flight Center. YYY thanks the NASA Postdoctoral Program for her fellowship.

DATA AVAILABILITY

The data underlying this article will be shared on reasonable request to the corresponding author.

REFERENCES

Anderson C. M., Nna-Mvondo D., Samuelson R. E., McLain J. L., Dworkin J. P., 2018, ApJ, 865, 1
Bernstein M. P., Sandford S. A., Allamandola L. J., 1997, ApJ, 476, 932
Brouillet N., Schilke P., 1993, A&A, 277, 381
Cordiner M. A. et al. 2019, ApJ, 870, L26
Crowley J. N., Sodeau J. R., 1989, J. Phys. Chem., 93, 3100
Danger G., Rimola A., Mrad N. A., Duvernay F., Roussin G., Theule P., Chiavassa T., 2014, Phys. Chem. Chem. Phys., 16, 3360
de Kok R. J., Teanby N. A., Maltagliati L., Irwin P. G. J., Vinatier S., 2014, Nature, 514, 65
Dello Russo N., Khanna R. K., 1996, Icarus, 123, 366
Dohnalek Z., Kimmel G. A.,Ayotte P., Smith R. S., Kay B. D., 2003, J. Chem. Phys., 118, 364
Dulmage W. J., Lipscomb W. N., 1951, Acta Crystallogr., 4, 330
Fedoseev G., Scirè C., Baratta G. A., Palumbo M. E., 2018, MNRAS, 475, 1819
Fresneau A., Danger G., Rimola A., Duvernay F., Theulé P., Chiavassa T., 2015, MNRAS., 451, 1649
Gerakines P. A., Bray J. J., Davis A., Richey C., 2005, ApJ, 620, 1140
Gerakines P. A., Hudson R. L., 2020, ApJ, 901, 1

Gerakines P. A., Moore M. H., Hudson R. L., 2004, Icarus, 170, 204
Giulano B. M., Escribano R. M., Martin-Doménech R., Dartois Muñoz, Caro G. M., 2014, A&A, 565, A108
Hassner A., Stern M., Gottlieb H. E., Frolow F., 1990, J. Org. Chem., 55, 2304
Hudgins D. M., Sandford S. A., Allamandola L. J., Tielens A. G. G. M., 1993, ApJS, 86, 713
Hudson R. L., Ferrante R. F., 2020, MNRAS, 492, 283
Hudson R. L., Loeffler M. J., Ferrante R. F., Gerakines P. A., Coleman F. M., 2020, ApJ, 891, 1
Hudson R. L., Loeffler M. J., Gerakines P. A., 2017, J. Chem. Phys., 146, 0243304
Hudson R. L., Moore M. H., 2004, Icarus, 172, 466
Hudson R. L., Moore M. H., Gerakines P. A., 2001, ApJ, 550, 1140
Huebner W. F., Snyder L. E., Buhl D., 1974, Icarus, 23, 580
Jamieson C. S., Chang A. H. H., Kaiser R. I., 2009, Adv. Space Res., 43, 1446
Jiménez-Escobar A., Giuliano B. M., Muñoz Caro G. M., Cernicharo J., Marcelino N., 2014, ApJ, 788, 19
Lellouch E. et al. 2017, Icarus, 286, 289
Masterson C. M., Khanna R. K., 1990, Icarus, 83, 83
Moore M. H., Ferrante R. F., Moore W. J., Hudson R. L., 2010, ApJS, 191, 96
Moore M. H., Hudson R. L., 2003, Icarus, 161, 486
Noble J. A., Theule P., Borget F., Danger G., Chomat M., Duvernay F., Mispelaer F., Chiavassa T., 2013, MNRAS, 428, 3262
Pézolet M, Savoie R., 1969, Can. J. Chem., 47, 3041
Quinto-Hernandez A., Wodtke A. M., Bennett C. J., Kim Y. S., Kaiser R. I., 2011, J. Phys. Chem. A, 115, 250
Rachid M. G., BrunkenN., de Boe D., Fedoseev G., Boogert A. C. A., Linnartz H., 2021, A&A, 653, A116
Satorre M. A., Domingo M., Millán C., Luna R., Vilaplana R., Santonja C., 2008, Planet. Space Sci. 56, 1748
Schloerb F. P., Kinzel W. M., Swade D. A., Irvine W. M., 1986, ApJ, 310, L55
Snyder L. E., Buhl D., 1971, ApJ, 163, L47
Swain M. R. et al. 2021, AJ, 161, 213
Swanepoel R., 1983, J. Phys. E: Sci. Instrum., 16, 1214
Theule P., Borget F., Mispelaer F., Danger G., Duvernay F., Guillemin Chiavassa T., 2011, A&A, 534, A64
Tokunaga A. T., Beck S. C., Geballe T. R., Lacy J. H., Serabyn E., 1981, Icarus, 48, 283
Tomlin S. G., 1968, J. Phys. D: Appl. Phys., 2, 1667
Uyemura M., Maeda S., 1972, Bull. Chem. Soc. Japan., 45, 1081
Venkatesh C. G., Rice S. A., Narten A. H., 1974, Science, 186, 927
Westley M. S., Baratta G. A., Baragiola R. A., 1998, J. Chem. Phys., 108, 3321
Wu Y., Wu C. Y. R., Chou S., Lin M., Lu H., Lo J., Cheng B., 2012, ApJ, 746, 175
Yarnall. Y. Y., Gerakines P. A., Hudson R. L., 2020, MNRAS, 494, 4606

This paper has been typeset from a TEX/LATEX file prepared by the author.